Oligocene and Miocene metamorphism, folding, and low-angle faulting in northwestern Utah

ROBERT R. COMPTON *Department of Geology, Stanford University, Stanford, California 94305*
VICTORIA R. TODD *U.S. Geological Survey, Menlo Park, California 94025*
ROBERT E. ZARTMAN, CHARLES W. NAESER *U.S. Geological Survey, Denver, Colorado 80225*

ABSTRACT

An area of 3,000 km² in and around the Grouse Creek Mountains and the Raft River Mountains exposes Precambrian, Paleozoic, and Triassic sedimentary rocks that were folded several times and displaced tens of kilometres on low-angle faults. Overturned folds and local imbrications indicate transport westward and northward during two episodes of metamorphic deformation and transport eastward after metamorphism. Metamorphic grade increases downward in the allochthonous sheets and autochthon and increases westward in the autochthon. Mineral grains are flattened into the horizontal plane, and shear strains increase upward, suggesting that the deformations were caused by gravity acting on a broadly heated dome. Rb-Sr dating of granitic plutons affected by the deformations indicates that (1) the area is underlain by adamellite, about 2.5 b.y. old, in which deformation decreased progressively downward; (2) the first metamorphic deformation probably ended before 38.2 ± 2.0 m.y. ago; and (3) the second metamorphic deformation was still underway 24.9 ± 0.6 m.y. ago.

High-grade allochthonous rocks that lie on low-grade parts of the autochthon indicate as much as 30 km of eastward transport after metamorphism. Parts of the dome sagged to form broad basins 12 m.y. ago, and the coarse sediments and tuffs that accumulated in them were overrun by allochthonous sheets measuring at least 11 by 19 km. Two Rb-Sr mineral isochrons and several fission-track ages indicate that some parts of the area cooled below 400 °C only 10 m.y. ago.

INTRODUCTION

The area studied is one of many in the region that expose low-angle faults of Mesozoic or Tertiary age; it is also one of about 20 localities where metamorphism and deformation were partly concurrent (Fig. 1). The map shows the great extent of these features but also presents a problem in interpreting them. The localities west of the belt of upthrusts are shown as separate dots because each is a mountain range surrounded by extensive alluvium. Folds and faults are superbly exposed in the ranges, but most are too complex to be connected reliably across the broad intervening basins. The belt of upthrusts, which is exposed more continuously, provides ample evidence of major eastward thrusting in Late Cretaceous and early Tertiary time, but contemporaneous tectonic features have been dated in only a few localities to the west (Hose and Blake, 1976; A. Snoke, 1974, oral commun.). Isotopic data from the western localities suggest a wide range of igneous rock ages, few of which have been attached firmly to tectonic events. A major problem is that K-Ar ages have been variably reset by Cenozoic heating. Nonetheless, the regional history has been interpreted by several persons (Misch, 1960; Roberts and others, 1965; Armstrong and Hansen, 1966; Armstrong, 1968b, 1972; Roberts, 1968; Hose and Danes, 1973; and Roberts and Crittenden, 1973). These histor are too varied to review here, but some events pertinent to o study have been assigned ages so consistently as to seem firm dated: (1) the Grouse Creek–Raft River area lay in the hinterla of a broad belt of west-to-east thrusting (or sliding) during Cret geous and possibly Late Jurassic time; (2) metamorphism in the gion was concurrent with deformation during the early part of t period only; and (3) starting no later than middle Tertiary time, entire region underwent extension and consequent high-angle fau ing, so that thrusting must have ceased.

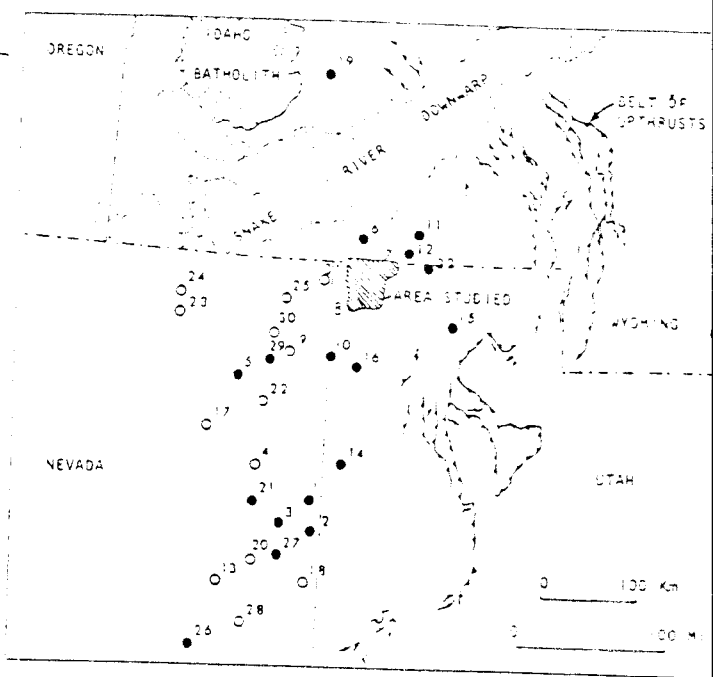

Figure 1. Tectonic features near area studied. Open circles = place where low-angle faults of Mesozoic or Tertiary age have been reported solid circles = places where metamorphic rocks were involved in deforma tion. 1, Ahlborn (1973); 2, Hazzard and Turner (1957), Misch and Haz zard (1962); 3, Young (1960); 4, Misch (1960), Hazzard and Turne (1957); 5, Howard (1966), Kistler and Willden (1969); 6, Armstrong (1968a); 7, Compton (1969, 1972); 8, Todd (1973); 9, Thorman (1970) 10, Woodward (1967), O'Neill (1969); 11 and 12, Anderson (1931); 13 Moores and others (1968); 14, Nelson (1966, 1969), Nolan (1935); 15, Ol son (1956); 16, Schaeffer and Anderson (1960); 17, Willden and others (1967); 18, Whitebread (1966), Lee and others (1970); 19, Dover (1969); 20, Misch (1960); 21, Woodward (1964); 22, Misch (1960); 23, Kerr (1962); 24, Fagan (1962); 25, Riva (1970); 26, Cebull (1970); 27, Drewes (1967); 28, Tchanz and Pampeyan (1970); 29, Thorman (1970); 30, Oversby (1972); 31, Slack (1974); 32, Peace (1956). Thrust faults are from King (1969).

Geological Society of America Bulletin, v. 88, p. 1237–1250, 13 figs., September 1977, Doc. no. 70903.

The dates determined in this study therefore seemed surprising, as did the directions of tectonic transport during metamorphism. In brief, our data indicate that metamorphism and folding in the Grouse Creek–Raft River area were going on as recently as 20 m.y. ago, that metamorphic flow and low-angle faulting were mainly northward and westward rather than eastward, that some allochthonous sheets traveled 30 km eastward after metamorphism, and that allochthonous sheets were emplaced both on Eocene(?) and older sedimentary and volcanoclastic rocks. We present our age data here and briefly describe structural relations [illegible]

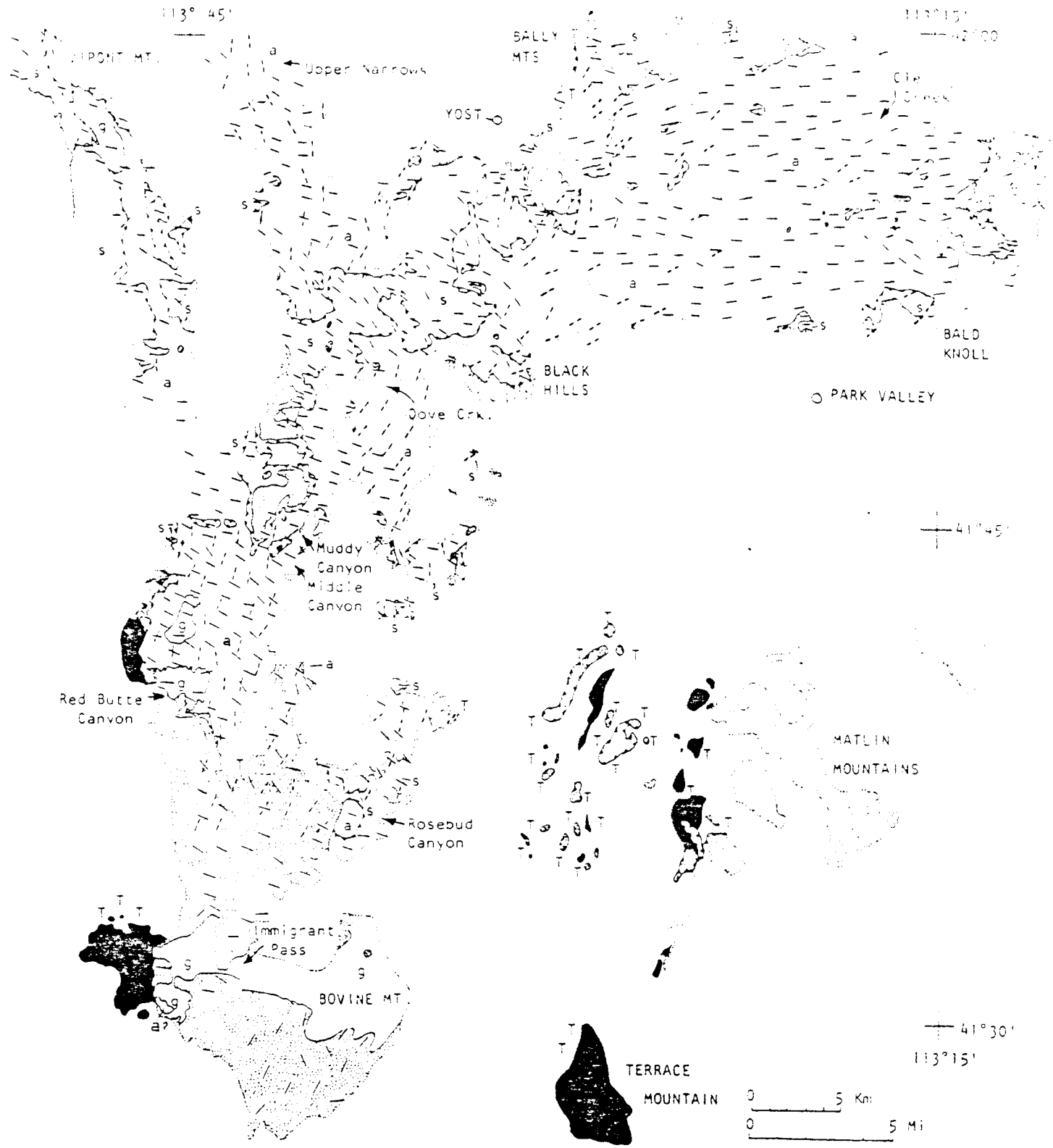

Figure 2. Structure map of Grouse Creek Mountains (north-south outcrop), Raft River Mountains (east-west outcrop), and vicinity. High-angle faults have been omitted. Black = upper allochthonous sheet; dots = middle sheet (and subsidiary sheets derived from it); s = lower sheet; a = autochthon; g = Tertiary granitic bodies. Dotted boundaries = depositional contacts with Cenozoic rocks; T = allochthonous sheets on Tertiary beds. Heavy dashes show axial trends of first metamorphic folds and lineations; thin unbroken lines show trends of second metamorphic folds and lineations.

maps and many lithologic and structural details are available (Compton, 1972, 1975; Todd, 1973).

ROCK UNITS AND LOW-ANGLE FAULTS

The Raft River Mountains expose two major allochthonous sheets that lie one above the other on an autochthon consisting mainly of Precambrian rocks. The Grouse Creek Mountains are similarly composed but include a third, still higher sheet along their western flank (Fig. 2). The Matlin Mountains and other low hills east of the Grouse Creek Mountains expose one or more north-northeast–striking, westward-dipping low-angle faults along which sheets of variably metamorphosed upper Paleozoic limestone and sandstone were carried over thick unmetamorphosed limestone and sandstone of similar age (V. R. Todd, unpub. data). In many places, these thin sheets were emplaced on upper Miocene tuffaceous sandstone and conglomerate (Fig. 2). The faults are exposed discontinuously for a distance of at least 19 km from north to south and for 11 km from east to west. Similar sheets lie on Tertiary beds at the north end of the Bally Mountains and at several localities in the Grouse Creek Mountains (Fig. 2). Fossils collected by Stanford field students at one of the latter localities include gastropods that were studied and assigned a late Miocene age by James E. Firby (1973, written commun.).

Deformed upper Miocene beds show that the Raft River Mountains formed as a doubly plunging east-trending anticline in Pliocene time and that the Grouse Creek Mountains formed at about the same time by arching and high-angle faulting. Erosion has exposed the autochthon to depths of 900 m in both ranges but has left enough klippen and peripheral patches of the allochthonous sheets so that they can be projected confidently over most of the mapped area.

Although folded in detail, the allochthonous sheets and autochthon are rudely stratified and were more or less horizontal before the mountain ranges formed. Figure 3 shows their total stratigraphic succession as well as the typical positions of the principal low-angle faults. Recumbent folding locally inverted the sequence, and low-angle faulting attenuated it and locally repeated it, but most of the rock units in the figure are generally present in the order shown.

Figure 3, however, is not a stratigraphic column. The thicknesses shown are all maximal for the area but are probably much less than the original sedimentary thicknesses, except for units younger than Mississippian. Solid-state flow caused considerable thinning, as shown by flattened grains and schistose fabrics that generally lie parallel to the subhorizontal layers. This effect varied considerably from place to place and is locally extreme: along the eastern flank of the central Grouse Creek Mountains and the adjoining southern flank of the Raft River Mountains, the total thickness of all units between the basal adamellite and the Fish Haven (?) Dolomite is commonly only 100 m.

Another important cause of thinning was faulting along surfaces that cut across stratigraphic units at low angles, displacing strata of the hanging wall onto older rocks. This is shown on a large scale by the middle sheet, which emplaced the upper part of the Mississippian or the lower part of the Pennsylvanian on Ordovician rocks throughout the north half of the area but includes progressively older Paleozoic units as it is traced southward in the Grouse Creek Mountains (Fig. 4). The feature cannot be a moderately faulted unconformity beneath an onlapping sequence because all of the units are lithologically the same as they are elsewhere in the region. The relation thus implies many tens of kilometres of displacement of the middle sheet. The middle sheet is also subdivided by subsidiary low-angle faults that produced similar but less extreme effects.

The fault at the base of the lower sheet locally rises from the schist of Stevens Spring to the schist of Mahogany Peaks or the marble of the Pogonip Group. The lower allochthonous sheet is cut out entirely in part of the eastern Raft River Mountains, where the Oquirrh Formation lies directly on the autochthon. Subsidiary imbricate thrusts that have locally emplaced older units over younger are associated with strongly overturned folds, as described in the next section.

FOLDS AND LINEATIONS

At least three sets of folds formed during metamorphism, and a fourth, which may locally be divided into several sets, formed after metamorphism. All of the folds plunge at low angles in most places. Axes of the oldest folds define a broad arc that swings from east-northeast in the Raft River Mountains to north, even northwest, in the Grouse Creek Mountains (Fig. 2). Almost all the folds are overturned toward the convex (northwest) side of the arc. Exceptions are east-overturned folds at the southern end of the Grouse Creek Mountains, which may not be continuous with folds to the north.

Axes of the second set of metamorphic folds trend northwest to due west in the Grouse Creek Mountains and approximately west in the Raft River Mountains. At scattered localities in the central Grouse Creek Mountains, west-trending metamorphic folds have overprinted northwest-trending folds. Almost all folds of the second set are overturned to the north. Exceptions are northwest-trending metamorphic folds in the lower, and particularly in the middle, allochthonous sheets in the central Grouse Creek Mountains that are overturned to the southwest. Still younger, scarce metamorphic folds (not shown in Fig. 2) trend northeast and are overturned toward the southeast, and in parts of the central Raft River Mountains late metamorphic folds of this trend are overturned toward the northwest.

The metamorphic folds range from upright to recumbent, most being strongly overturned. The largest are recumbent and measure 0.5 to 1.5 km from anticlinal hinge to adjoining synclinal hinge. These large folds are typically solitary or in couplets, with rock layers extending nearly unaffected for many kilometres in front of the folds or behind them. Hinges of the most prominent folds in the Raft River Mountains can be followed for 22 km in the autochthon. Only a few folds of comparable size occur elsewhere, but the numbers of smaller folds increase exponentially with decreasing fold size, such that folds with wavelengths of about 1 m can be seen at many localities (except in the upper allochthonous sheet), and folds smaller than 5 mm are so abundant as to impart a pervasive and characteristic linear ridging or striping to surfaces of many quartzite and marble layers. Other linear elements parallel to these small folds include flattened and elongated pebbles, triaxial quartz and calcite grains, prismatic kyanite and hornblende grains, elongated mica plates, and open-space fillings (typically calcite) on two sides of pyrite crystals.

The postmetamorphic folds (not shown in Fig. 2) have a variety of forms and trends, suggesting that movements at that stage were complex and localized. The largest of these folds in the western Raft River Mountains are probably of the same age as the youngest metamorphic folds in the central Grouse Creek Mountains. Their sense of transport could be determined 14 km southwest of Yost, where a fan-shaped array of large folds that are overturned generally toward the east is cut by imbricate thrusts with the same sense of transport (Compton, 1972). Six kilometres northeast of Yost, folds of approximately the same age have strongly deformed the middle low-angle fault and subsidiary low-angle faults in the lower sheet.

Recumbent north-trending folds in the middle allochthonous sheet of the central Grouse Creek Mountains are probably of the same age as those just mentioned but formed where metamorphism was still in its waning stages. They measure as much as 0.5 km from anticlinal hinge to synclinal hinge, are overturned to the east, and are cut by imbricate thrusts displaced toward the east.

Postmetamorphic folding also affected the autochthon widely but by no means universally. The folds range from slight rolls and crimps to open chevron folds overturned to the east. None have

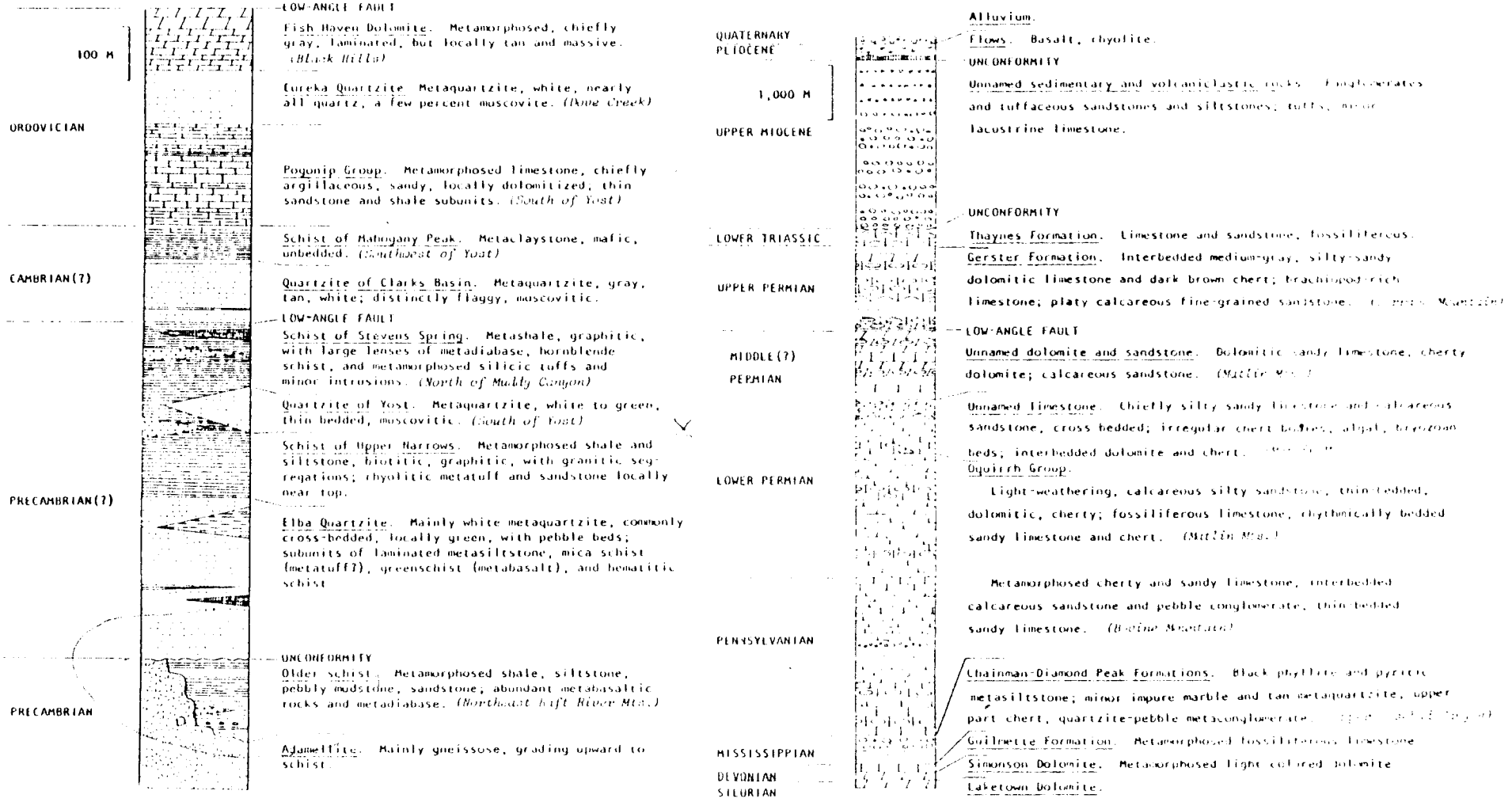

Figure 3. Sequence of rock units in area studied. Not shown are Tertiary granitic rocks, which intruded units as young as Permian. Note that scale on right-hand column is one-tenth that on left.

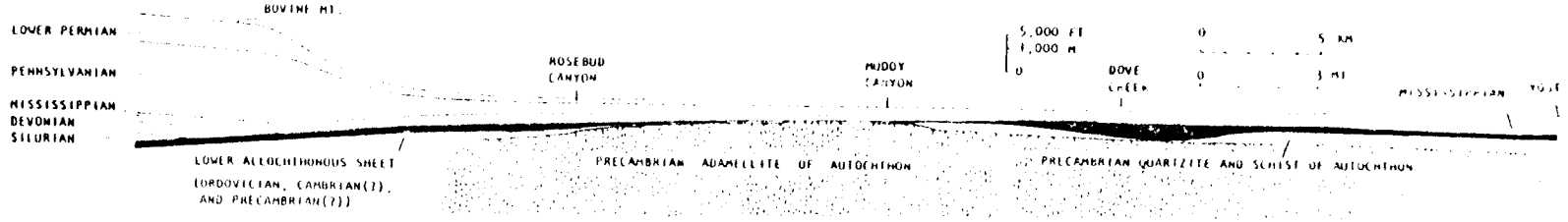

Figure 4. Partly reconstructed north-south vertical section from west end of Raft River Mountains to south end of Grouse Creek Mountains, at natural scale, showing stratigraphic composition of middle allochthonous sheet. Lower sheet and units in autochthon are shown virtually as they are now, but units in middle sheet south of Rosebud Canyon have been reconstructed from greatly folded and faulted fragments.

wavelengths of more than 1 m, and all trend between N30°W and N30°E.

METAMORPHIC VARIATIONS

Vertical and lateral variations in metamorphic grade due to temperature differences help greatly in interpreting the deformations. The general vertical variations are as follows: (1) the upper allochthonous sheet is not metamorphosed; 2) the middle sheet is not metamorphosed in some places, but in others shows an increasing degree of low-grade metamorphism downward; and 3) the lower sheet and the autochthon are metamorphosed, with metamorphic grades generally increasing downward. Table 1 lists the principal mineral assemblages for the highest grade part of each unit. Because parts of the sheets were displaced after metamorphism, the tabulated section is a reconstructed metamorphic sequence for the most heated part of the area at the peak of prograde metamorphism. Textures indicate that the minerals in each assemblage coexisted at that time, whether or not true equilibria were attained. Except for the fine-grained schists of the Oquirrh and Chainman or Diamond Peak Formations, most mineral grains are between 0.05 and 5 mm in diameter.

The lateral variations in metamorphic grade are simplest in the autochthon: the highest grade rocks are in the western part of the area and the lowest grade in the eastern part. The pre-adamellite schists have not been studied in enough places to be meaningful,

TABLE 1. MINERAL ASSEMBLAGES IN HIGHEST GRADE PARTS OF ROCK UNITS IN GROUSE CREEK AND RAFT RIVER MOUNTAINS

Rock unit	Original rock	Metamorphic minerals
Oquirrh Formation	Silty limestone	Calcite, dolomite, quartz, colorless mica, relict detrital feldspars
Diamond Peak Formation	Shale	Colorless mica, quartz, biotite, chloritoid, graphite
Fish Haven(?) Dolomite	Dolomite	Dolomite, quartz, colorless mica, tremolite, relict K-feldspar
Eureka(?) Quartzite	Sandstone	Quartz, colorless mica
Pogonip Group	Sandy, clayey limestone	Calcite, dolomite, zoisite, calcic plagioclase, colorless mica, biotite, quartz
Schist of Mahogany Peaks	Mafic shale	Colorless mica, staurolite, garnet, biotite, quartz
Quartzite of Clarks Basin	Feldspathic sandstone	Quartz, colorless mica, kyanite, chloritoid (locally biotite and garnet)
Schist of Stevens Spring	Shale	Colorless mica, quartz, biotite, garnet, oligoclase, graphite
	Basalt	Green hornblende, plagioclase
	Granite porphyry	Quartz, K-feldspar, oligoclase, colorless mica, biotite
Schist of Upper Narrows	Shale	Biotite, colorless mica, quartz, K-feldspar, oligoclase
Elba Quartzite	Feldspathic sandstone	Quartz, colorless mica, biotite, K-feldspar, plagioclase
Older Precambrian units	Adamellite	Oligoclase, orthoclase, quartz, biotite
	Gabbro	Green hornblende, intermediate plagioclase, garnet, quartz
	Shale	Biotite, quartz, oligoclase, garnet (altered metasomatically during late metamorphism to assemblages with kyanite, staurolite, andalusite, sillimanite)

Note: Minerals listed in order of decreasing abundance.

but in the west the amphibolite consists of hornblende, intermediate plagioclase, and garnet and in the east of finer grain hornblende, epidote, albite, and chlorite. The Precambri adamellite, which has been studied more extensively, has the pr grade assemblage listed in Table 1 in the Grouse Creek Mountain and it has the assemblage microcline–quartz–albite–white mic epidote–biotite throughout the east half of the Raft River Mou tains. The adamellite is distinctly gneissose in the Grouse Cre Mountains, with few igneous textural relics, but changes gradua eastward to less foliated varieties with many igneous textural reli

Lateral changes of the Elba Quartzite have been studied in 1 thin sections. Where the rock shows its highest grade assemblag in the central part of the Grouse Creek Mountains, quartz grai are nearly equant polyhedra, and white mica and biotite form d tinct plates. Toward the east, biotite disappears, quartz grains a more flattened and irregular, and white mica is finer grained a more irregular. Near the east end of the Raft River Mountai quartz and feldspar grains larger than 0.5 mm commonly have t shapes of relict sand grains, some even preserving diagenetic ov growths. Quartz grains also show an increasing amount of po crystallization strain toward the eastern part of the area.

In the schist immediately above the Elba Quartzite, biotite coarser (0.2 to 0.7 mm) in the western part of the area than in t eastern part (where it is 0.01 to 0.05 mm), and the degree of gran lation during recrystallization increases toward the east. Schist the Upper Narrows in the eastern part of the Raft River Mountai has assemblages such as chlorite–white mica–albite–quartz a albite-quartz-biotite-epidote, which contrast with the western a semblages (Table 1).

The lower allochthonous sheet also varies laterally in metamo phic grade, being highest in grade in the western Raft River Mou tains, about 12 km northeast of the highest grade part of the a tochthon (Fig. 5). Especially recognizable are variations within t Pogonip Group, which is coarsely porphyroblastic marble where

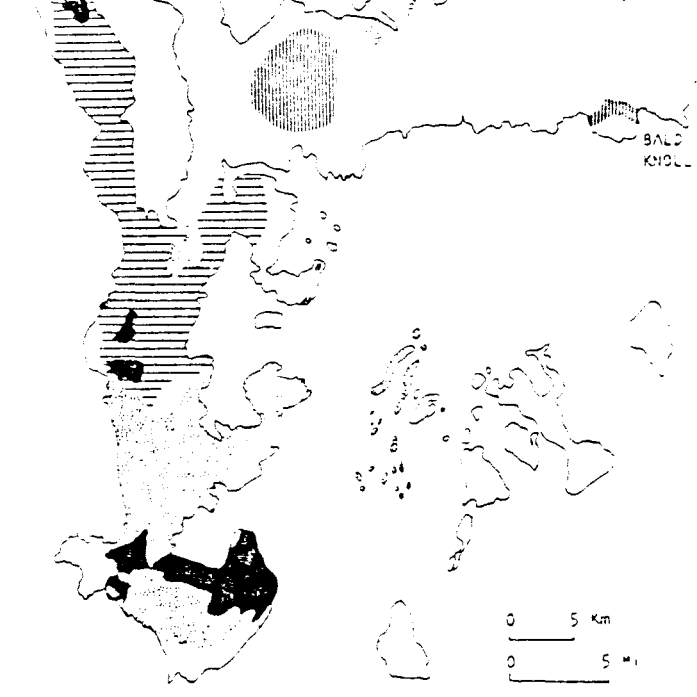

Figure 5. Locations of highest grade parts of autochthon (horizon lines) and of lower allochthonous sheet (vertical lines). Dots show wh Oquirrh Formation of middle sheet is metamorphosed. Tertiary plute show in black. Outcrop is same as that of Figure 2.

Figure 4. Partly reconstructed north–south cross section through scale, showing stratigraphic composition of middle allochthonous sheet in middle sheet south of Rosebud Canyon have been reconstructed fr

ver sheet and units in autochthon are shown virtually as they are now, and most ly folded and faulted fragments.

contains high-grade minerals (Table 1) but changes to the southwest and to the east. White mica is the only new metamorphic mineral in marble of intermediate grade, and the lowest grade rocks, near the east end of the Raft River Mountains, contain abundant relics of sedimentary grains, including shredded white mica. An important exception is a high-grade outlier at Bald Knoll (Fig. 5). Variations in other Cambrian(?) and Ordovician units are consistent; the schist of Mahogany Peaks loses its large staurolite and garnet grains to the south, east, and west, and white mica grains in the Eureka(?) Quartzite and Fish Haven(?) Dolomite become smaller in the same directions, again except for the outlier at Bald Knoll.

The Mississippian rocks of the middle sheet are metamorphosed everywhere, but the Oquirrh Formation is metamorphosed only locally (Fig. 5). Gradations within the Oquirrh from metamorphosed to unmetamorphosed rocks are well exposed in the central and southern Grouse Creek Mountains.

In view of the systematic variations of metamorphic grade in the autochthon and the allochthonous sheets, and considering the thinness of the lower sheet, the distribution of high-grade rocks shown in Figure 5 is provocative. The high-grade rocks of the lower sheet at Bald Knoll are 30 km east of the high-grade part of the autochthon and lie on some of the lowest grade rocks of the autochthon. Likewise, the metamorphosed Oquirrh of the middle sheet lies on low-grade rocks of the lower sheet along the north side of the Raft River Mountains and in the central Grouse Creek Mountains. Unmetamorphosed Oquirrh rocks lie directly on the most metamorphosed part of the lower sheet, and, near Vipont Mountain, they lie only 100 m, vertically, from the highest grade rocks of the autochthon. These relations indicate major low-angle faulting after metamorphism or late in metamorphism, with a large resultant transport from west to east. The isolated occurrence of higher grade rocks in the lower sheet at Bald Knoll also indicates separate movement of a subsidiary part of the lower sheet. Separate movements of subsidiary sheets are also suggested by metamorphic relations around Tertiary stocks of the Grouse Creek Mountains, as will be discussed when the dating of the stocks is described.

DATING OF PRECAMBRIAN ADAMELLITE

Precambrian adamellite was sampled for dating near the east end of the Raft River Mountains and in the central Grouse Creek Mountains, in the lowest and highest grade parts, respectively, of the autochthon. Exposures elsewhere show that similar adamellite extends under all or most of the mapped area, and studies by Armstrong (1968a) of the Albion Range show that similar rock extends at least 38 km northward from the western part of our area.

Clear Creek Canyon

Adamellite is well exposed from its contact with older rocks, 5 km from the mouth of Clear Creek Canyon (Fig. 2), to the canyon head, 6 km to the southwest (Compton, 1975). Five samples for dating were collected at various places along the canyon, starting 1 km west of the contact with the older schist and extending 4 km southwest. Throughout the east half of the Raft River Mountains the rock is typically homogeneous and nearly granular, with a weak metamorphic foliation and lineation. Feldspar phenocrysts, as long as 3 cm, are typically sparse but locally abundant; otherwise the grain size is typically 1.5 mm. Contacts with the older rocks are sharp in most places, although metashales are feldspathized locally for as much as 10 m from the adamellite. In several places the adamellite grades outward to a porphyroaphanitic border zone against older mafic igneous rocks. The irregular boundary is apparently a chilled margin, suggesting a shallow emplacement of the adamellite in this part of the area.

The adamellite is dominantly hypidiomorphic granular, with plagioclase distinctly subhedral although altered to albite, white mica, and Fe-poor epidote. Metamorphism deformed and recrystallized quartz, recrystallized biotite into scaly aggregates, recrystallized single sphene grains into aggregates, and formed epidote in the foliated parts of the rock. Small amounts of postmetamorphic alteration are shown everywhere by minute cracks filled with very fine grained Fe-smectite(?).

The analytical data are plotted on a Rb-Sr diagram in Figure 6. The samples define only a poor linear array, and a least-squares regression line yields an age of 2,180 ± 190 m.y. The high $^{87}Sr/^{86}Sr$ intercept (0.764) may reflect either a later disturbance of the Rb-Sr chemistry or a crustal contribution to the initial strontium in the magma. We cannot distinguish uniquely between these two possibilities, but the generally older ages of 2.5 b.y. or greater for basement rock throughout the Wyoming province (Condie, 1969; Reed and Zartman, 1973) and the substantial degree of alteration shown by these rocks causes us to suspect postcrystallization open-system conditions. Furthermore, the adamellite has appreciably higher Rb/Sr ratios than other analyzed Precambrian rocks in the vicinity — a factor often found to correlate with age modification during subsequent metamorphism and weathering.

Fission-track ages on the Precambrian adamellite and associated rocks of the Raft River Mountains indicate metamorphism of Tertiary age followed by exceptionally rapid cooling. Sphene and apatite from adamellite sample CC-1 (Table 2) gave annealing ages of 20 ± 10 m.y. for sphene and 20 ± 4 m.y. for apatite; the ± values are 2σ and $\lambda_f = 6.85 \times 10^{-17}$ yr^{-1}). A second sample is from the older schist 100 m above an intrusive contact with Precambrian adamellite at lat 41°55'46"N, long 113°19'59"W, which is 2.6 km southeast of locality CC-1. This sphene gave an age of 10.2 ± 1.9 m.y., and the apatite 12.4 ± 2.4 m.y. A sample of Pogonip marble metamorphosed to schist consisting mainly of epidote, quartz, potassium feldspar, biotite, calcite, and colorless mica was collected 30 m above the base of the lower allochthonous sheet, at the northwest edge of the Black Hills (lat 41°50'18"N, long 113°33'31"W). The apatite has a very low uranium content (0.4 ppm) but gave an age of 46 ± 26 m.y. for one determination and 66 ± 32 m.y. for another.

Annealing of fission tracks in sphene takes place at temperatures of about 400 °C (Calk and Naeser, 1973); if the temperatures are sustained for geologically significant periods — greater than 10^6 yr. Apatite is annealed of fission tracks if temperatures above 100 °C are sustained for 10^6 yr or more (Naeser and Faul, 1969). The fission-track ages of the sphenes thus suggest that the rocks in and around Clear Creek Canyon were at metamorphic temperatures as recently as Miocene time. The quartzites in that part of the range have strongly preferred crystallographic fabrics that are coaxial

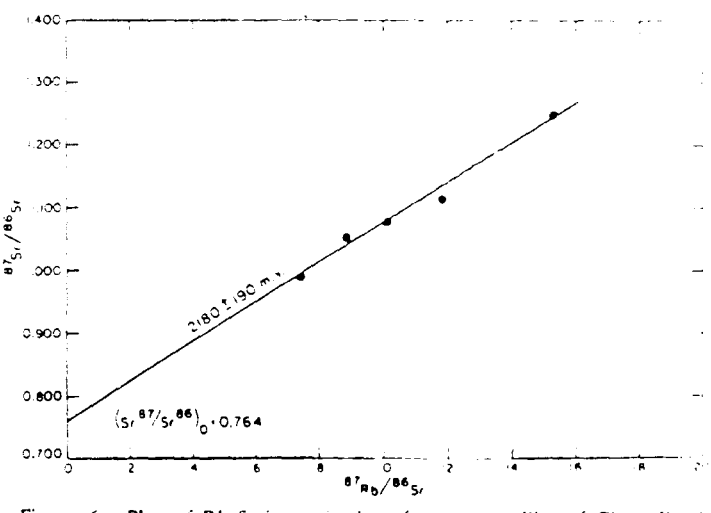

Figure 6. Plot of Rb-Sr isotopic data from adamellite of Clear Creek Canyon, Raft River Mountains. Data are listed in Table 2.

with large recumbent folds of the second metamorphic set, and they also show abundant features produced by posterystallization strain. Evidently, the east-west–trending folds were still forming in Miocene time, and the close similarity of the sphene and apatite ages for each rock suggests that the rocks then cooled rapidly.

The older ages for the apatites from the Black Hills cannot be interpreted firmly because they are very approximate and because the sample is from an allochthonous sheet that probably moved many kilometres after metamorphism. The data show, nonetheless, that some parts of the terrain cooled well before others. This is supported by data of Armstrong and Hansen (1966, p. 123), who reported K-Ar ages of biotites from two autochthonous rocks of the Raft River Mountains. A sample of Precambrian adamellite from Clear Creek Canyon, about 2.5 km southwest of our CC-1, gave an age of 57 + 8/−3 m.y., and a sample of older schist (possibly schistose adamellite) from Big Hollow, 5 km east of the Black Hills, gave an age of 38 + 6/−2 m.y. for one biotite split and an age of 41 + 6/−2 m.y. for a second split.

Central Grouse Creek Mountains

The contact between the Precambrian adamellite and younger quartzites and schists is a metamorphosed unconformity throughout the Raft River and the northern Grouse Creek Mountains, but in the central Grouse Creek Mountains, adamellite appears to intrude quartzite and schist. In Muddy Canyon, thin sills of adamellite gneiss and schist occur between beds of Elba Quartzite, and bedded quartzite forms concordant inclusions in the upper 100 m of adamellite. The upper contact of the adamellite cuts across upper Precambrian(?) units of the autochthon into the lower allochthonous sheet at a low angle (Fig. 4). The youngest unit intruded by Precambrian adamellite is Cambrian(?) quartzite of Clarks Basin. Partly granitized, contorted schist inclusions are notably abundant in the upper part of the adamellite, suggesting that the missing section was in part downfolded and incorporated by mobilized adamellite.

The Elba Quartzite thins from 215 m about 2.5 km north of Muddy Canyon to 6 m in the north wall of the canyon (Fig. 4). Equally striking are the thinning by metamorphic flow and low-angle faulting of all metasedimentary rocks of the autochthon and of the lower allochthonous sheet above the area of mobilized adamellite.

The adamellite of the central Grouse Creek Mountains shows a systematic change in texture upward, from coarse- and medium-grained gneiss in the lowest exposures to fine-grained gneiss and schist in the upper part, about 920 m above the base of the range. Textures indicate simultaneous deformation and recrystallization. Similarly, numbers of relict igneous grains decrease upward, and phengitic white mica, quartz, albite, iron-poor epidote, and sphene increase upward, as the higher temperature oligoclase-orthoclase-quartz-biotite assemblage is replaced. Under the Elba Quartzite is a zone about 6 m thick in which medium-grained adamellite grades upward through feldspathic schist of adamellite composition to phengite-quartz-albite schist (Fig. 7). It is noteworthy that these schists contain the same accessory minerals, principally allanite and dark red-brown metamict zircon, as the less altered adamellite below. Locally, the metamict zircon in the schists bears partial jackets of colorless birefringent zircon.

Adamellite in the central Grouse Creek Mountains was folded twice during metamorphism. Recrystallized mineral aggregates form two prominent lineations oriented parallel to the two fold sets. The earlier lineation (northeast to north-northwest–trending) consists of quartzofeldspathic rods, elongate biotite aggregates, and parallel crenulations 0.5 to 1 cm wide lying in the foliation plane, in deeper lying exposures. Wavelengths of the crenulations and widths of the linear mineral aggregates decrease upward; near the top of the range they are typically only a few millimetres wide. This decrease is part of an increase in deformation and recrystallization. In deeper lying rocks, the second (northwest to west-northwest) lineation consists of subhedral biotite grains that cross the earlier coarser biotite aggregates and, in thin section, appear to have recrystallized from them. In the reconstituted upper shell of the adamellite and in rocks surrounding the two small Tertiary stocks on the west side of the range (roughly the upper 185 m of adamellite), the second lineation consists of quartz-feldspar rods, biotite aggregates, and distinct crenulation, and the first lineation is present only as faint wrinkling. These relations suggest two important points: (1) strain and recrystallization increased upward in the

TABLE 2. Rb-Sr ISOCHRON AGES OF WHOLE-ROCKS FROM PRECAMBRIAN ADAMELLITE, NORTHWESTERN UTAH

Sample no.	Lat (N)	Long (W)	Rb (ppm)	Sr_n (ppm)	$^{87}Rb/^{86}Sr$	$^{87}Sr/^{86}Sr$	Age (m.y.)*
Clear Creek Canyon							
CC-1	41°56′50″	113°21′07″	297.2	75.5	11.85	1.113	
CC-2	41°55′57″	113°22′49″	275.4	110.7	7.40	0.9908	
CC-3	41°56′00″	113°22′43″	257.6	86.9	8.87	1.055	2,180 ± 190
CC-5	41°56′31″	113°22′02″	271.1	80.3	10.12	1.077	
CC-6	41°56′43″	113°21′32″	293.7	58.5	15.30	1.248	
Central Grouse Creek Mountains							
GW-67-19A	41°41′21″	113°44′20″	83.4	144.2	1.684	0.7679	
GW-67-19B	41°41′21″	113°44′20″	111.7	138.3	2.360	0.7998	
GW-67-19C†	41°41′21″	113°44′20″	240.9	152.4	4.629	0.8263	
GW-67-21	41°41′32″	113°44′23″	166.2	98.2	4.988	0.8883	
GW-67-26	41°41′23″	113°41′22″	101.5	148.2	1.998	0.7902	
GW-67-28	41°40′18″	113°44′34″	124.9	141.3	2.582	0.8111	
10W 21-1A†	41°45′10″	113°41′19″	184.7	77.3	6.990	0.8208	2,510 ± 170
10W 21-1B†	41°45′10″	113°41′19″	150.2	28.8	15.24	0.8048	
10W 21-4A	41°45′03″	113°41′10″	126.7	109.3	3.396	0.8222	
10W-21-4B	41°45′03″	113°41′10″	141.3	121.9	3.399	0.8368	
10W-23-1	41°43′36″	113°42′04″	129.8	109.2	2.488	0.8456	
10W-23-2A	41°43′33″	113°42′23″	170.0	138.0	3.613	0.8391	
10W-23-2B	41°43′33″	113°42′23″	123.4	136.7	2.638	0.8014	

*Calculated from least-squares regression method of York (1966). See graphic representation of these data in Figures 6 and 8. Decay constant: $\lambda_d = 1.39 \times 10^{-11}\ yr^{-1}$.

†Samples not included in calculation of age.

adamellite when the first folds and lineations formed, and (2) recrystallization of minerals during the second folding reached a maximum in rocks adjacent to, and lying above, the Tertiary stocks.

In the central part of the Grouse Creek Mountains, Precambrian adamellite is interlayered with lesser amounts of granodiorite, tonalite, and leucocratic gneiss. Suites of these four rocks were collected from three areas for dating. Three medium-grained gneisses representative of deeper exposures are from Middle Canyon (Fig. 2). Six fine-grained samples, typical of the upper part of the gneiss, were collected on Ingham Peak, which is 4 km southwest of Middle Canyon. Four samples of metasomatically altered gneiss and schist are from Muddy Canyon, where the intrusive-appearing contact of Precambrian adamellite with the Elba Quartzite is well exposed (Fig. 7). The samples are listed below by locality.

Middle Canyon. Sample 10W-23-1 is medium-grained tonalite gneiss, 10W-23-2a is medium- to coarse-grained adamellite gneiss (the typical adamellite of the gneiss complex), and 10W-23-2b is medium-grained muscovitized granodiorite gneiss.

Ingham Peak. Samples 9W-97-19a, b, and c were collected from a typical outcrop of interlayered adamellite and mafic gneiss from the highest peak of the central Grouse Creek Mountains. Sample 9W-97-19c is from a thin gneissic granitic pegmatite layer in fine-to medium-grained adamellite gneiss, the rock of sample 9W-97-19b. Sample 9W-97-19A is fine- to medium-grained granodiorite gneiss from an adjoining mafic layer and was collected 10 cm from 9W-97-19b. Sample 9W-97-21 is adamellite gneiss from a site about 610 m north of 9W-97-19, 9W-97-26 is muscovitized adamellite gneiss collected 92 m north of 9W-97-19, and 9W-97-28 is leucoadamellite gneiss from a site about 2,200 m south of 9W-97-19. All three samples are fine to medium grained.

Muddy Canyon. Samples 10W-21-1a and 1b are phengite-quartz schists collected adjacent to an inclusion of Elba Quartzite 1.8 m below the contact between mobilized Precambrian adamellite and Elba Quartzite. The inclusion consists of several thin beds, in all 10 cm thick, that lie parallel to the foliation of the schist. Sample 10W-21-1b was 0.6 m above the quartzite inclusion, and sample 10W-21-1a lay about 0.5 m below it. Samples 10W-21-4a and 4b were collected about 7.5 m below the contact between the Elba Quartzite and Precambrian adamellite. Sample 10W-21-4b is fine- to medium-grained muscovitized adamellite gneiss, and sample 10W-21-4a is a 30-cm, concordant fine- to medium-grained leucoadamellite dike in 10W-21-4b. This series of samples is representative of the border zone of the Precambrian adamellite in which muscovitized adamellite gneiss grades upward through feldspathic schist to phengite-quartz schist (Fig. 7).

Although we originally interpreted the adamellite of the central Grouse Creek Mountains to be Phanerozoic, the Rb-Sr diagram (Fig. 8) reveals an old Precambrian age. A whole-rock isochron age of 2,510 ± 170 m.y. was obtained from our data, excluding the two schistose rocks (10W-21-1a and 1b) associated with the metaquartzite in Muddy Canyon and the pegmatite (9W-97-19c) from Ingham Peak. The ten remaining samples show approximately the same degree of scatter as those from the Clear Creek Canyon locality despite their being more metamorphosed. Indeed, the somewhat older age and lower $^{87}Sr/^{86}Sr$ intercept seem to suggest a more restricted isotope redistribution in these rocks. In particular, the closely adjoining adamellite gneiss (9W-97-19b) and granodiorite gneiss (9W-97-19a) gave no evidence of strontium isotope homogenization between the two layers. The granitic pegmatite layer (9W-97-19c), which intrudes the adamellite gneiss, however, either has undergone exchange or possibly is slightly younger.

The only samples that have obviously undergone major chemical reconstitution are the phengite-quartz schists (10W-21-1a and 1b) within the immediate border zone between the basement rocks and the overlying Elba Quartzite. The schistose rocks have similar strontium isotope compositions but appreciably higher Rb/Sr ratios and, consequently, younger ages than the gneiss. We do not know whether this effect arises from metamorphic differentiation in the extremely sheared rock or from a mechanical mixing with the younger mantling rocks. The other, less deformed samples (10W-21-4a and 4b) from Muddy Canyon show little disturbance of their Rb-Sr systems even though they have recrystallized. The relations between the rheomorphic and chemical responses of the basement rock have not been adequately resolved by this study; they remain an interesting and important subject for further work.

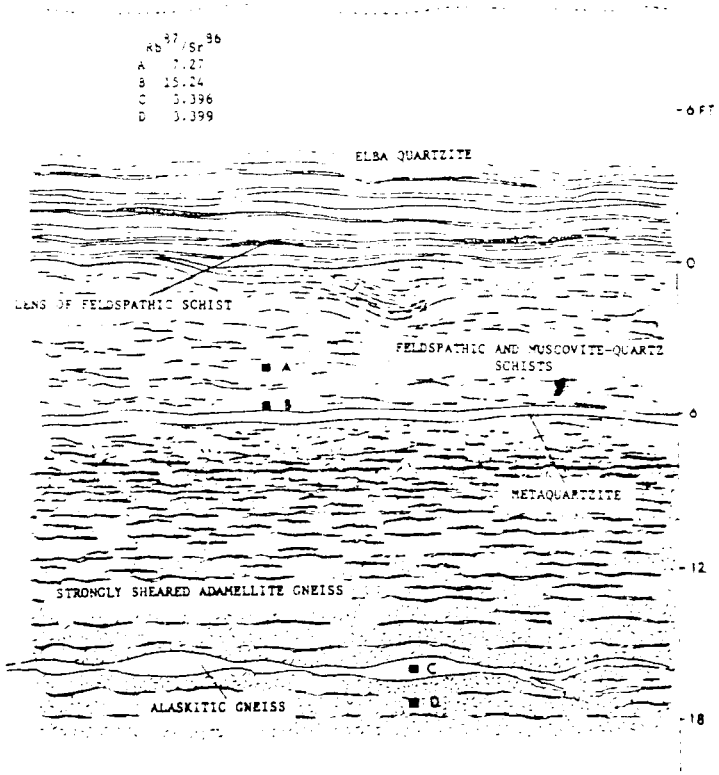

Figure 7. Diagrammatic section through upper part of Precambrian adamellite and Elba Quartzite in Muddy Canyon, showing gradation from gneiss to schist, interposition of schistose adamellite in quartzite, and isotope ratios determined from samples from positions indicated.

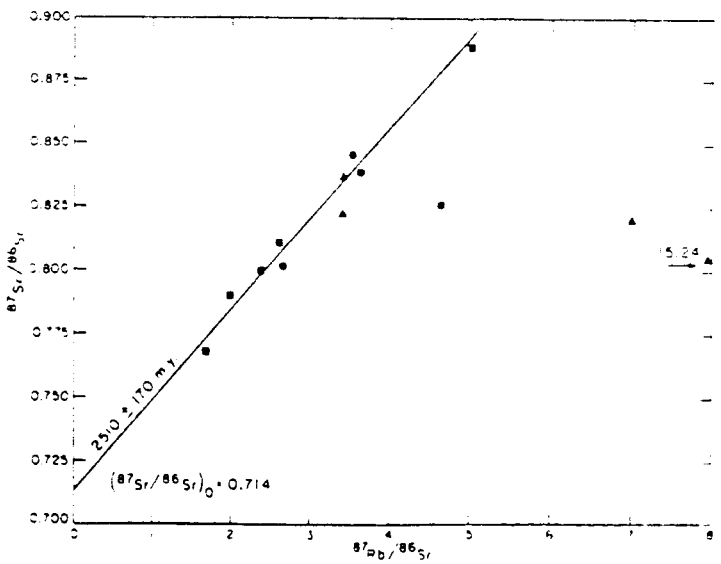

Figure 8. Plot of Rb-Sr isotope data from gneissose to schistose adamellite of central Grouse Creek Mountains. Data are listed in Table 2. Circles = Middle Canyon; squares = Ingham Peak; triangles = Muddy Canyon.

In order to determine whether the individual mineral grains had equilibrated isotopically among themselves within a hand specimen, the plagioclase, microcline, and biotite were analyzed from two of the samples (9W-97-21 and 10W-23-2a). The results, together with those of the whole-rock analyses, are given in Table 3. On this scale the minerals have rather recently attained internal homogenization of their strontium isotopes. Only the biotite with its very high Rb/Sr ratio has evolved isotopically to a significant extent after homogenization. Assuming that the biotite did indeed fully participate in the exchange, we were able to calculate biotite whole-rock ages of 11.9 and 8.0 m.y. on these samples. If our assumptions are correct, the results indicate that chemical mobility and, presumably, elevated temperatures persisted in late Miocene time in the central Grouse Creek Mountains, a situation similar to that indicated by the fission-track ages in the eastern Raft River Mountains.

DATING OF TERTIARY INTRUSIONS

The Grouse Creek Mountains expose several young granitic bodies, shown individually in Figures 2 and 5: (1) at Vipont Mountain, in the northwest corner of the mapped area, (2) two closely spaced stocks in and near Red Butte Canyon in the central part of the range, and (3) the large, probably multiple intrusion near the south end of the range at Immigrant Pass.

Vipont Mountain Intrusion

The lineated granodiorite and adamellite of Vipont Mountain intruded all of the rock units in the lower allochthonous sheet but did not intrude the middle sheet. The country rocks dip 5° to 20° west, and the upper contact of the intrusion is roughly concordant with them, being emplaced mainly below the quartzite of Clarks Basin but breaking across this unit toward the south and connecting with thick sills in marble of the Pogonip Group and the schist of Mahogany Peaks (Fig. 9). The upper part of the intrusion and the associated sills somehow engulfed and assimilated much of the stratigraphic section, especially the schist of Mahogany Peaks and the upper part of the quartzite of Clarks Basin. Possibly because of this, the upper part of the intrusion is banded by variably biotitic adamellites, many bearing garnet, whereas the main body of the intrusion is homogeneous garnet-free granodiorite.

Age relations of the intrusion to deformational features are well exposed. The first set of metamorphic folds is developed locally in the country rocks above the intrusion but nowhere in the intrusion. All of the body is lineated parallel to the second set of metamorphic folds and associated lineations in the country rocks. The country rocks are exceptionally high grade near the intrusion, the Pogonip marble bearing garnet and pyroxene, and the schist of Mahogany Peaks being converted to oligoclase-quartz-sillimanite-muscovite-biotite gneiss in which sillimanite and biotite are lineated parallel to the second metamorphic folds. The rocks of the middle allochthonous sheet lying on these high-grade rocks are metamorphosed little, if at all, so this part of the middle sheet must have been emplaced after the intrusion cooled almost completely.

The highest lying adamellite sills are converted in several places to sheets of dark blastomylonite in which rounded relics of igneous feldspar are surrounded by recrystallized, swirled trains of fine-grained quartz, biotite, and feldspar. Because these rocks are strongly lineated parallel to overturned folds of the second metamorphic set, it appears that the allochthonous sheet shown in Figure 2 rode over the intrusion during the second folding episode. This relation indicates low-angle faulting during the second metamorphic folding.

The localities of the analyzed rocks are shown in Figure 9, and their textural and structural features are as follows: sample 4,

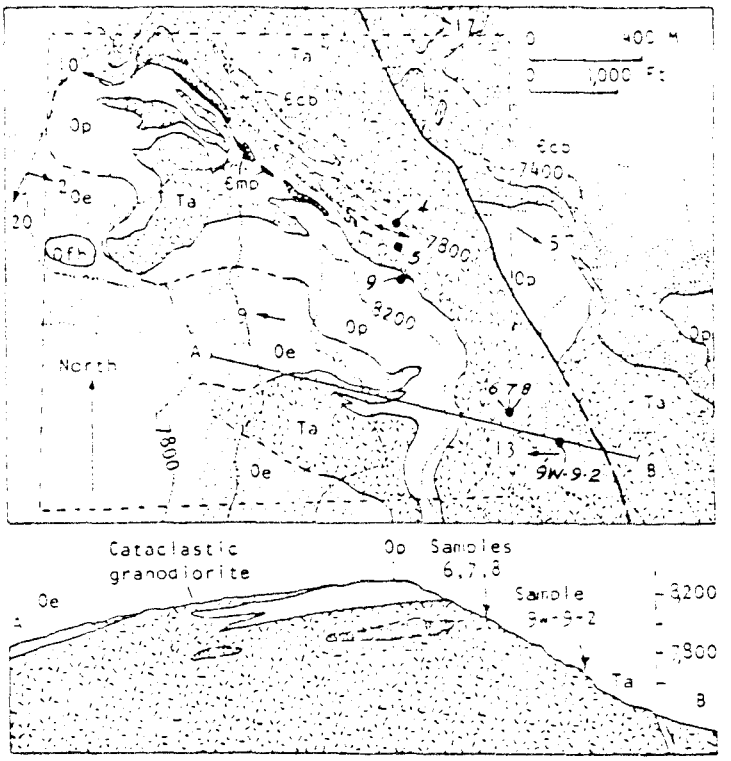

Figure 9. Geologic map and vertical section showing locations of samples used in Rb-Sr studies of Vipont Mountain intrusion. Contours (dotted) and outline of Sec. 8, T. 15 N., R. 17 W., are from the Cotton Thomas Basin 15' quadrangle. Arrows show plunges of folds and lineations. Ecb = quartzite of Clarks Basin (Cambrian?) (heavy stipple); Emp, = schist of Manogany Peaks (Cambrian?) (black); Op = marble of Pogonip Group (Ordovician) (unpatterned), Oe = Eureka(?) Quartzite (Ordovician) (light stippie); Ofh = Fish Haven(?) Dolomite (Ordovician) (unpatterned); and Ta = Tertiary adamellite and granodiorite (cross-tracked). Cross section, which is enlarged from map, has horizontal and vertical scales equal.

TABLE 3. Rb-Sr BIOTITE–WHOLE-ROCK AGES FROM PRECAMBRIAN ADAMELLITE, NORTHWESTERN UTAH

Sample no.	Lat (N)	Long (W)	Mineral	Rb (ppm)	Sr_n (ppm)	$^{87}Rb/^{86}Sr$	$^{87}Sr/^{86}Sr$	Age m.y.*
9W-97-21	41°41'32"	113°44'23"	Plagioclase	184	140	3.9	0.8880	
			K-feldspar	361	120	9.0	0.8897	
			Whole rock	166.2	98.2	4.99	0.8883	11.9 ± 0.2
			Biotite	1,056	3.0	1,056	1.063	
10W-23-2A	41°43'33"	113°42'23"	Plagioclase	100	203	1.5	0.8348	
			K-feldspar	294	160	5.5	0.8426	
			Whole rock	170.0	138.0	3.61	0.8391	8.0 ± 0.5
			Biotite	917.0	11.6	232.7	0.861	

* Calculated as biotite–whole-rock pairs. Decay constant: $\lambda_\beta = 1.39 \times 10^{-11}\ yr^{-1}$.

TABLE 4. Rb-Sr ISOCHRON AGES OF WHOLE ROCKS FROM TERTIARY INTRUSIONS, NORTHWESTERN UTAH

Sample nos.	Lat N	Long W	Rb (ppm)	Sr_n (ppm)	$^{87}Rb/^{86}Sr$	$^{87}Sr/^{86}Sr$	Age (m.y.)
Vipont Mountain							
9W-9-2	41°56'52"	113°48'46"	140	240	1.6	0.7217	
4	41°57'17"	113°49'11"	124.8	171.8	2.105	0.7235	
5	41°57'15"	113°49'10"	150.6	94.7	4.613	0.7308	
6	41°56'56"	113°48'53"	87.7	421.0	0.603	0.7123	Indeterminate
7	41°56'56"	113°48'53"	226.4	20.8	31.64	0.7306	
8	41°56'56"	113°48'53"	231.2	26.5	25.33	0.7276	
9	41°57'12"	113°49'09"	45.2	1,182	0.111	0.7104	
Red Butte Canyon							
9W-47-2A	41°39'47"	113°45'27"	193.0	93.1	6.01	0.7169	
9W-47-2B	41°39'47"	113°45'27"	235.5	5.22	131.2	0.7592	
9W-47-2C	41°39'47"	113°45'27"	240.6	2.36	298.7	0.8180	
9W-47-2D	41°39'47"	113°45'27"	235.5	7.44	92.0	0.7450	24.9 ± 0.6
9W-47-9	41°39'49"	113°45'32"	335.7	22.2	43.8	0.7294	
9W-47-10	41°39'49"	113°45'32"	265.7	8.22	93.5	0.7427	
Immigrant Pass							
9W-39-1	41°30'52"	113°44'59"	103.8	285	1.05	0.7102	
9W-39-2	41°31'01"	113°45'07"	246.2	6.34	112.3	0.7716	
9W39-3	41°30'58"	113°45'05"	362.1	7.16	146.4	0.7860	
9W-40-2	41°32'07"	113°45'58"	210.0	40.7	14.94	0.7184	38.2 ± 2.1
13W-167-3	41°31'44"	113°41'48"	205.0	15.4	38.60	0.7282	
13W-167-4	41°31'37"	113°41'57"	152.2	56.4	7.82	0.7140	

* Calculated from least-squares regression method of York (1966). See graphical representation of these data in Figures 10 and 12. Decay constant: $\lambda_\beta = 1.39 \times 10^{-11}$ yr^{-1}.

lineated adamellite from a 2.5-m sill in quartzite of Clarks Basin; sample 5, lineated adamellite from a thick sill near or at the base of the marble of the Pogonip Group; sample 6, typical lineated granodiorite from the lower more homogeneous part of the intrusion; sample 7, muscovite-bearing leucoadamellite, part of a 1-m-thick vertical dike in the rock of sample 6, moderately lineated parallel to the folds of the second metamorphic set; sample 8, muscovitic leucoadamellite from another part of the same dike as sample 7; sample 9W-9-2, granodiorite much like sample 6 but more deformed; and sample 9, marble of the Pogonip Group, 30 m south of the locality of sample 5.

An attempt to define an age for the granitic body from Vipont Mountain has not been successful. Most of the analytical data given in Table 4 and shown in Figure 10 crudely mimic an ~500-m.y. isochron, but the pluton intrudes rocks younger than that. The leucoadamellite dike rock, which, from its high Rb/Sr ratio, appears to have undergone considerable differentiation relative to the main igneous mass, seemingly records a much younger age. Field and petrographic relations suggest that the ~500-m.y. age was largely inherited by the igneous rocks during assimilation of lower Paleozoic rocks of the lower allochthonous sheet. If the Rb and Sr so derived were not significantly fractionated in the process, an approximate lower Paleozoic isochron age could be transferred to the granite. The range in $^{87}Rb/^{86}Sr$ ratio so incorporated would impart a highly variable initial strontium isotope composition to the magma. Assuming, for example, a Tertiary age for the intrusion, the $^{87}Sr/^{86}Sr$ ratio would vary between 0.710 and 0.730. Because of this uncertainty in initial strontium isotope composition, we cannot precisely date even the two apparently differentiated leucoadamellite samples (7 and 8). If these rocks experienced no posterystallization disturbance, we can only broadly establish their age as lying between 0 and 50 m.y., depending on what initial isotopic composition we choose to assume. This extreme involvement of the allochthonous and perhaps the autochthonous rocks in the generation of the magma without subsequent thorough homogenization and differentiation does not exist in the other Tertiary intrusions to be discussed.

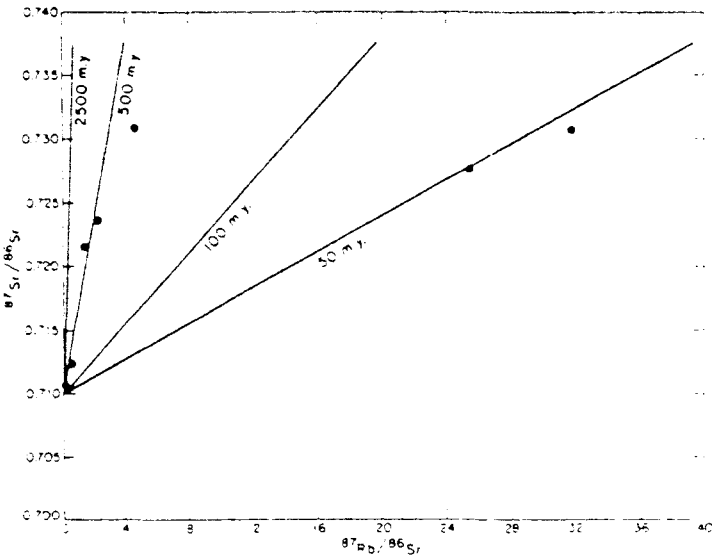

Figure 10. Plot of Rb-Sr isotope data from Vipont Mountain intrusion, northern Grouse Creek Mountains. Data are listed in Table 4.

Stocks of Red Butte Canyon

The two small Tertiary stocks on the west side of the central Grouse Creek Mountains are cupolas of an adamellite body that lies close to the surface throughout the central part of the range, judging from the distribution of dikes and metamorphism of the surrounding rocks. The upper contacts of the stocks are broadly concordant with bedding in the westward-dipping, metamorphosed lower and middle allochthonous sheets and with foliation in the Precambrian adamellite. Discordant dikes of alaskite and aplite from the stocks are abundant in the Precambrian adamellite and in the lower and middle allochthonous sheets near the stocks.

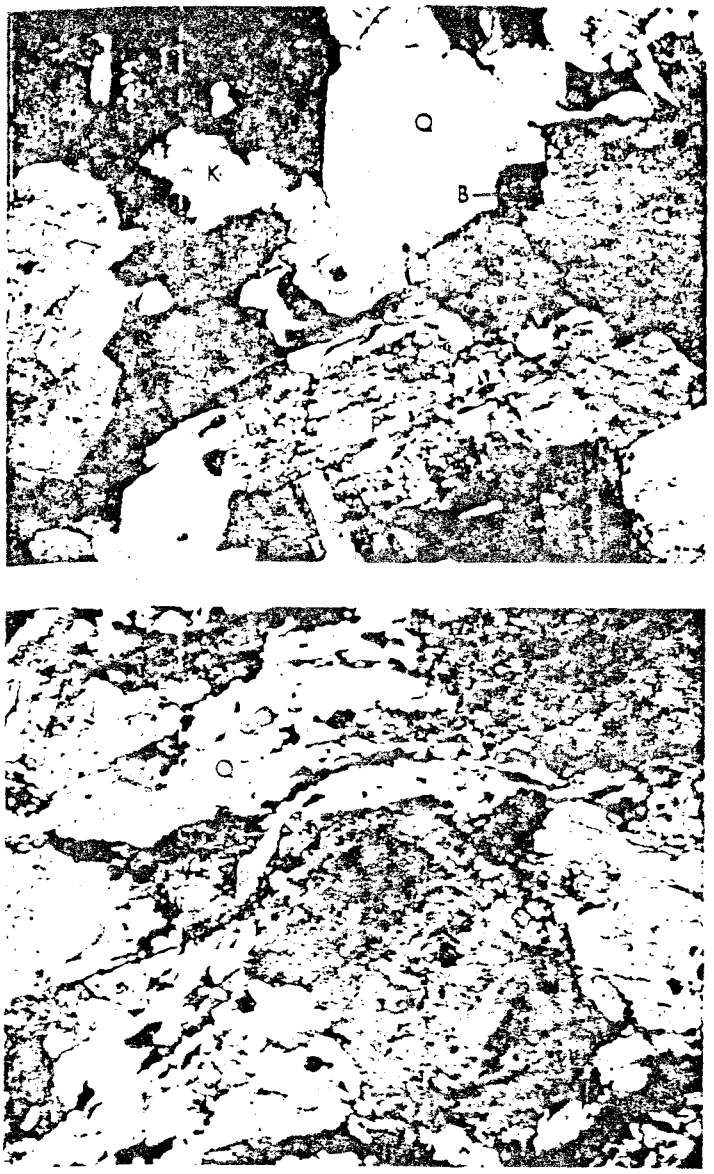

Figure 11. Photomicrographs, each of 1-cm area, showing textural variations in adamellite of pluton of Red Butte Canyon. Top: weakly foliated and lineated adamellite with subhedral plagioclase (P), unstrained quartz (Q), potassium-feldspar (K), and biotite (B). Bottom: strongly lineated gneiss 200 m below base of middle allochthonous sheet, with quartz in fine aggregates (Q), and biotite reduced in size and partly altered to chlorite and sphene.

Rotated and partly altered inclusions of wall rocks occur in the Tertiary adamellite near its margins.

The Precambrian adamellite and rocks of the middle sheet show evidence of marked thermal metamorphism over a distance of about 0.75 km from the stocks. Recrystallization of mineral grains in the Precambrian adamellite parallel to axes of the second metamorphic folds was most intense near the Tertiary stocks. Cherty dolomite of the middle sheet was converted to tremolite, dolomite, muscovite, and diopside(?) in a contact aureole centered approximately over the stocks, indicating that post intrusive displacement was not large on this part of the middle fault. In contrast, the upper sheet, locally only 200 m above the Tertiary body, shows no thermal metamorphism.

Aligned biotite grains define a weak foliation that disappears gradually toward the interior of the adamellite body. A faint west-northwest to east-west lineation composed of quartz and feldspar grains and biotite aggregates can be seen on foliation surfaces and

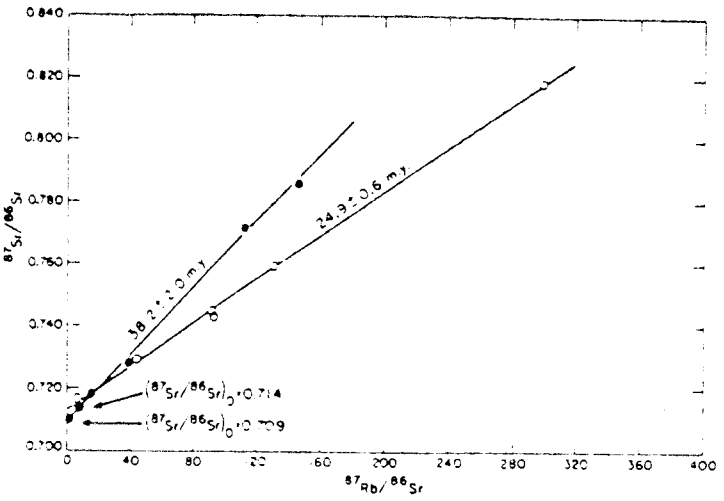

Figure 12. Plots of Rb-Sr isotope data from stocks of Red Butte Canyon and from Immigrant Pass intrusion, Grouse Creek Mountains. Data are listed in Table 4. Open circles = Red Butte Canyon; solid circles = Immigrant Pass.

in some thick dikes of alaskite and aplite. These fabric elements parallel the foliation and second metamorphic lineation in the surrounding metamorphic rocks, including the Precambrian gneiss. The biotite fabric and lineation are moderate to strong within 46 m of the Precambrian gneiss (Fig. 11). Over a horizontal distance of 460 m under the middle allochthonous sheet, Tertiary adamellite in Red Butte Canyon is strongly gneissose and markedly lineated by microfolds and mineral grains. A zone of mylonitized adamellite about 3 m thick occurs immediately beneath the middle sheet. Microfolds and strong mineral lineation in the mylonite are parallel to west-northwest–trending folds in overlying tectonitic, thermally metamorphosed dolomite of the middle sheet. Thus, the intrusion and crystallization of the Tertiary adamellite coincided with movement on the middle low-angle fault and with the second metamorphic folding, but predated emplacement of the upper allochthonous sheet.

Except for the marginal zone, the adamellite is a medium-grained, hypidiomorphic, equigranular rock consisting of oligoclase, quartz, and potassium feldspar in approximately equal volume and roughly 5% biotite. Coarse-grained adamellite with sparse, euhedral, 2- to 4-cm potassium feldspar phenocrysts occurs locally in the inner part of the body. Abundant magmatic features include euhedral feldspar phenocrysts, synneusis aggregates, and delicate euhedral oscillatory zoning in plagioclase. The core of the body appears structureless, suggesting that it solidified after deformation had ceased. Leucoadamellite, alaskite, and aplite in irregular bodies and dikes ranging from several millimetres to 100 m in thickness occur in and around the stocks.

All dated samples of the Tertiary body were collected from the southernmost part of the southern stock about 0.8 km north of upper Ingham Creek. Sample 9W-47-2A (illustrated in Fig. 11) is homogeneous, weakly foliated biotite adamellite; 9W-47-2B is fine-grained muscovitic adamellite from a 30-cm-thick, sharp-walled dike in rock of sample 9W-47-2A; 9W-47-2C is a muscovitic aplite dike, 15 cm thick, intruded into rock of sample 9W-47-2B; and 9W-47-2D is aplite from several 6-cm-thick dikes approximately 60 m from the collection site of samples 9W-47-2B and 2C. Sample 9W-47-9 is aplite from a dike 20 cm thick, and 9W-47-1D is from the center of a vertical aplite dike 1.2 m thick. Other samples of average adamellite had $^{87}Rb/^{86}Sr$ and $^{87}Sr/^{86}Sr$ ratios similar to that of 9W-47-2A.

The six samples from the southern stock define a whole-rock isochron age of 24.9 ± 0.6 m.y., with an initial $^{87}Sr/^{86}Sr$ ratio of 0.714 ± 0.002 (Table 4; Fig. 12). The ability to obtain so precise an

age on a body so young is attributable to the extremely high Rb/Sr ratios present in the differentiated leucoadamellite and aplite dike
ks. Also, even if the slight scatter observed in the isochron dia-
.m is a reflection of initial strontium isotope variability, the magma could not have been as heterogeneous as the one at Vipont Mountain. The initial $^{87}Sr/^{86}Sr$ ratio, however, does imply some crustal contribution to the magma, although the ratio is considerably lower than would be acquired solely from melting of the nearby Precambrian adamellite basement rocks.

The intimate association between the main adamellite body and the various dikes that cut it and the adjacent country rock implies a genetic and, presumably, a temporal relation. Thus, we feel confident that this late Oligocene age applies not only to the dikes but also to the entire intrusion and to the superimposed second metamorphic fabric. We further conclude from the lack of contact metamorphic effects in the upper allochthonous sheet that it had not moved into its present position at this time. This interpretation is compatible with field evidence showing allochthonous sheets resting upon upper Miocene beds (Fig. 2).

Fission-track data from the pluton strongly support the idea that even though the body was emplaced in late Oligocene time, it crystallized and cooled in Miocene time. One sample (13W-29-11) is from moderately gneissose adamellite from the northwest edge of the northern stock, about 3 m from the contact with Precambrian adamellite (lat 41°42′49″N, long 113°45′45″W). Zircon from this rock gave an age of 18.3 ± 1.9 m.y., and apatite gave an age of 13.7 ± 3.7 m.y. The second sample (9W-99-39) came from a dike of garnetiferous alaskite, 1 m thick, in the Precambrian adamellite about 25 m from the contact of the southern stock in upper Ingham Canyon (lat 41°39′50″N, long 113°44′46″W). The apatite from this rock gave an age of 18.9 ± 6.3 m.y. These data suggest that the pluton continued to be heated for many millions of years after it
stallized.

ımmigrant Pass Intrusion

The largest and least known of the Tertiary granitic bodies was named the Grouse Creek pluton by Baker (1959). It consists of a large eastern lobe and two smaller western lobes (Fig. 5). All of these intruded the middle allochthonous sheet, but the upper sheet is unmetamorphosed even where it is in contact with the western lobes, so that it must have been emplaced here after they cooled. The pluton cuts north- to northeast-trending folds in the middle sheet, folds interpreted to be of the first set. We have not yet established the age relation of the pluton to the younger set of metamorphic folds. Mapping to date indicates that the granitic rocks are not distinctly lineated. The ten thin sections examined, however, show considerable low-temperature strain, including kinking of plagioclase and biotite. A large (1 by 2 km) mass of Elba Quartzite in the southwest lobe (labeled a? in Fig. 2) has also been strained at low temperature.

All three lobes of the Immigrant Pass intrusion are mainly biotite granodiorite verging on adamellite. Textures are hypidiomorphic granular, with grains averaging 3 mm in diameter, although locally with scattered 1 to 2-cm grains. Garnetiferous leucoadamellite of about the same grain size forms thick dikes in the west half of the body and a broad zone along the west margin of the two western lobes. Diorite, syenodiorite, and similar rather mafic rocks are abundant in the small southwestern lobe. Aplite and pegmatite dikes are widespread and locally abundant in all the lobes.

Samples for isotopic dating were collected from each of the three lobes. Sample 9W-39-1 is from a freshly blasted roadcut in
mogeneous granodiorite typical of the central part of the southstern lobe; 9W-39-2 is from a nearby garnetiferous
ucoadamellite dike, 8 to 10 m thick, that intrudes the granodiorite; 9W-39-3 is from the finer grained part of an aplitic and pegmatitic leucoadamellite forming a 0.5- to 1-m-thick dike in typical granodiorite, 200 m northeast of the locality of 9W-39-1. Samples 13W-167-3 and 4 are dike rocks from the large eastern lobe of the pluton; 13W-167-3 is from a 0.7-m-thick dike of homogeneous aplite near the center of the lobe, and 13W-167-4 is from a 0.2-m-thick dike of porphyritic alaskite about 400 m distant from the other. The remaining sample, 9W-40-2, is from a 0.3-m-thick aplite dike in granodiorite typical of the northwestern lobe.

The six samples define a composite whole-rock isochron age of 38.2 ± 2.0 m.y. with an initial $^{87}Sr/^{86}Sr$ ratio of 0.7109 ± 0.0002 (Table 4; Fig. 12). This age, however, is controlled predominantly by the two samples of dike rock from the southwestern lobe of the pluton and should be applied strictly only to this locality. Although the other sample points lie close to the isochron, their low radiogenic enrichments and the uncertainties observed elsewhere in initial $^{87}Sr/^{86}Sr$ ratios combine to obscure an accurate interpretation. For example, the one analysis for a sample of the large eastern lobe plots equally well on the Red Butte Canyon isochron.

The present stage of the mapping also does not allow a determination of the relative ages of the three lobes. Possibly the late Eocene or early Oligocene age applies to the southwestern lobe only. Armstrong (1970) determined a K-Ar biotite age of 23.3 m.y. on granodiorite from the north end of the northwestern lobe, but it is not known whether this result reflects primary crystallization or later heating.

DISCUSSION

The fission-track and Rb-Sr data from the pluton in Red Butte Canyon set one firm date in the tectonic history: the second metamorphic deformation was still underway in late Oligocene time. A Miocene date for the end of metamorphism is suggested by the fission-track data from the autochthon in the eastern Raft River Mountains and by the Rb-Sr mineral isochrons for the Precambrian adamellite of the Grouse Creek Mountains.

The first metamorphic deformation probably ended before 38.2 ± 2.0 m.y. ago, for the intrusion at Immigrant Pass cuts through large folds that are probably of that deformation. We have no other dates on this deformation, but its metamorphic minerals, fold forms, and vertical distribution of strains are so similar to those of the second deformation as to suggest that the two followed one another closely.

Looking at the region broadly, the first deformation was directed at large angles, even 180°, to the west-to-east transport indicated by overthrusts in the late Mesozoic and early Tertiary thrust belt (Fig. 1). Activity in the thrust belt must thus have ended before the first metamorphic deformation, or else directions of transport varied greatly in the region. We have found no folds or other small-scale tectonic features older than those of the first metamorphic deformation. For example, countless pebbles and cobbles in Precambrian units are flattened and elongated into simple triaxial ellipsoids that lie parallel to the metamorphic fold axes, and these forms are otherwise only locally kinked on north-trending axes of the postmetamorphic folds.

Postmetamorphic deformation and igneous activity were widespread, variable, and locally of large magnitude. Tectonic transport during the period from about 20 to 12 m.y. ago was eastward, as shown by strongly overturned folds and by offsets of parts of the allochthonous sheets, some traveling as much as 30 km. These events led up to the deposition of the upper Miocene beds, which record voluminous volcanic activity and rapid erosion of the allochthonous sheets. Coarse detritus from unmetamorphosed Triassic, Permian, and Pennsylvanian units makes up the lower thousand or so metres of the sequence, and clasts of metamorphic rocks appear at higher levels. This clast stratigraphy is so consistent over the entire area as to suggest that the sediments accumulated in

broad basins and that the allochthonous sheets were not broken by high-angle faults with large vertical displacements. The upper Miocene beds were then folded on approximately north-trending axes, and parts of the middle and upper allochthonous sheets were emplaced onto them. Finally, the present ranges formed, probably in Pliocene time, and faults of basin-and-range type developed along the eastern front of the Grouse Creek Mountains and locally elsewhere.

With that much overview of the history, we can turn to the question of what caused it. Probably the most significant facts come from the dating and structural study of the Precambrian adamellite: (1) the entire area was underlain by a nearly flat-topped body of great strength and low porosity, from about 2.5 b.y. ago onward; 2) the metamorphic fabrics in the body, like those in the rocks above it, are dominantly horizontal or nearly so; and (3) the fabrics decrease in intensity downward — so rapidly in the least metamorphosed (eastern) part of the area as to be scarcely discernible 800 m below the top of the adamellite.

These facts are difficult to reconcile with horizontally directed compression of either the adamellite or the layered rocks above it, which tends to rule out thrusting during the period of metamorphism. The vertical distribution of strain also excludes infrastructure-suprastructure models, such as that proposed by Armstrong and Hansen (1966) for this same area.

A model proposed by Kehle (1970), on the other hand, seems suitable to the distribution of deformation. His model has three rock layers: a rigid basement, a ductile intermediate layer, and a less ductile upper layer. The layers remain immobile as long as they are horizontal or nearly so, but when they are tilted to some critical slope, gravity induces shear in the ductile layer. Rocks in the ductile layer thus flow laterally over the basement and carry the upper layer with them. For the area studied, the basement was the Precambrian adamellite, and the ductile layer included all the metamorphosed rocks above it — part of the autochthon, all of the rocks of the lower allochthonous sheet, and parts of the middle sheet. Figure 13 is a simplified diagram, similar to those used by Kehle, showing the relative amounts of displacive strain at various depths. The relation between the ductile layer and the overlying rocks is poorly known because of erosion, but it is probably a gradation.

Our case differs from Kehle's simple three-layer model in that major low-angle faults have developed. The lowest fault lies mainly in the graphitic schist of Stevens Spring, or at its upper contact, and the middle fault (which is apparently the one with the largest displacement) lies mainly in the metamorphosed organic shales of the Mississippian, or at their upper contact. Water and organic fluids were unquestionably produced in these units during thermal diagenesis and metamorphism. These facts fit the general mechanism proposed by Hubbert and Rubey (1959): the expelled fluids led to separation and nearly frictionless translation of the allochthonous sheets. At the several places where we can determine the direction of translation, it is the same as the sense of shear in the ductile rocks above and below the faults.

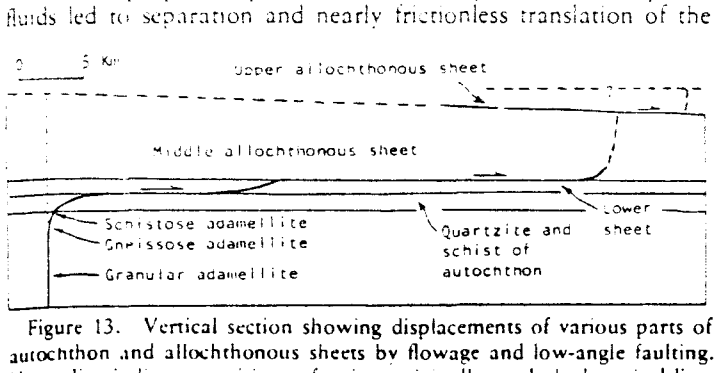

Figure 13. Vertical section showing displacements of various parts of autochthon and allochthonous sheets by flowage and low-angle faulting. Heavy line indicates positions of points originally on dashed vertical line. Strains are idealized to one movement plan. Actual slopes of surfaces are unknown. Vertical dimensions are approximate and are depicted to scale at time that deformation started.

It thus appears that both flow and faulting resulted from thermally induced changes and were probably driven by gravity. Indeed, it is plausible that the entire deformational system was caused by widespread heating and uplift. The greater degree of heating (metamorphism) in the part of the area where granitic plutons occur suggests that more extensive, subjacent plutons caused the heating as well as the uplift, perhaps forming a broad dome. The shape of the dome could have changed with time, thus providing an explanation for the changes in direction of flow and low-angle faulting as well as for the varied overturn of folds with depth and for the unequal cooling histories from place to place. The first set of metamorphic folds would represent the west and north sides of the dome during that deformation. The crest of the dome may have shifted to a position near Muddy Canyon during the second deformation, for the folds north of the canyon are overturned to the north whereas those in the middle and lower allochthonous sheets south of the canyon are overturned to the southwest. The crest would then have shifted to the west, leading to large-scale eastward transport at the close of metamorphism and afterward. Finally, the late Miocene basins suggest that large parts of the eastward-facing surface sagged at that time. Even so, the recent cooling dates, the contemporaneous volcanism, and the emplacement of subsidiary sheets on the upper Miocene rocks suggest that heating and deformation remained closely related until they ended, about 10 m.y. ago.

ACKNOWLEDGMENTS

Mapping by Stanford field classes in 1965, 1967, 1969, and 1973 contributed to our data and ideas, and the Bureau of Land Management, the U.S. Forest Service, and many ranchers aided the field studies. We thank Max Crittenden, Jr, for visits in the field and for his suggestions and general encouragement. Todd's field studies were financed by a Geological Society of America Research Grant and by a U.S. Geological Survey Postdoctoral Fellowship, and her petrographic materials were financed by a grant from the Shell Research Fund at Stanford University. Compton's work was supported in part by the U.S. Geological Survey. We thank Max Crittenden, Jr., and Fred K. Miller for reading and criticizing the paper.

REFERENCES CITED

Ahlborn, R. C., 1973, Tectonic and plutonic events in the Kern Mountains: Geol. Soc. America Abs. with Programs, v. 5, p. 1–2.

Anderson, A. L., 1931, Geological and mineral resources of eastern Cassia County, Idaho: Idaho Bur. Mines and Geology Bull. 14, 29 p.

Armstrong, R. L., 1968a, Mantled gneiss domes in the Albion Range, southern Idaho: Geol. Soc. America Bull., v. 79, p. 1295–1314.

——1968b, Sevier orogenic belt in Nevada and Utah: Geol. Soc. America Bull., v. 79, p. 429–458.

——1970, Geochronology of Tertiary igneous rocks, eastern Basin and Range province, western Utah, eastern Nevada, and vicinity, U.S.A.: Geochim. et Cosmochim. Acta, v. 34, p. 203–232.

——1972, Low-angle (denudation) faults, hinterland of the Sevier orogenic belt, eastern Nevada and western Utah: Geol. Soc. America Bull., v. 83, p. 1729–1754.

Armstrong, R. L., and Hansen, E., 1966, Cordilleran infrastructure in the eastern Great Basin: Am. Jour. Sci., v. 264, p. 112–127.

Baker, W. H., 1959, Geologic setting and origin of the Grouse Creek pluton, Box Elder County, Utah [Ph.D. thesis]: Salt Lake City, Univ. Utah, 175 p.

Calk, L. C., and Naeser, C. W., 1973, The thermal effect of a basalt intrusion on fission-tracks in quartz monzonite: Jour. Geology, v. 81, p. 189–198.

Cebull, S. E., 1970, Bedrock geology and orogenic succession in southern Grant Range, Nye County, Nevada: Am. Assoc. Petroleum Geologists Bull., v. 54, p. 1828–1842.

Compton, R. R., 1969, Thrusting in northwest Utah: Geol. Soc. America Abs. with programs for 1969, Pt. 3 (Rocky Mountain Sec.), p. 15.

——1972, Geologic map of the Yost quadrangle, Box Elder County, Utah, and Cassia County, Idaho: U.S. Geol. Survey Misc. Geol. Inv. Map I-672.

——1975, Geologic map of the Park Valley quadrangle, Box Elder County, Utah, and Cassia County, Idaho: U.S. Geol. Survey Misc. Geol. Inv. Map I-873.

Condie, K. C., 1969, Geologic evolution of the Precambrian rocks in northern Utah and adjacent areas: Utah Geol. and Mineralog. Survey Bull., v. 82, p. 71–95.

Dover, J. H., 1969, Bedrock geology of the Pioneer Mountains, Blaine and Custer Counties, central Idaho: Idaho Bur. Mines and Geology Pamph. 152, 61 p.

Drewes, Harald, 1967, Geology of the Connors Pass quadrangle, Schell Creek Range, east-central Nevada: U.S. Geol. Survey Prof. Paper 557, 93 p.

Fagan, J. J., 1962, Carboniferous cherts, turbidites, and volcanic rocks in northern Independence Range, Nevada: Geol. Soc. America Bull., v. 73, p. 595–612.

Hazzard, J. C., and Turner, F. E., 1957, Décollement-type overthrusting in south-central Idaho, northwestern Utah and northeastern Nevada: Geol. Soc. America Bull., v. 68, p. 1829.

Hose, R. K., and Blake, M. C., Jr., 1976, Geology and mineral resources of White Pine County, Nevada: Part 1, Geology: Nevada Bur. Mines and Geology Bull. 85, p. 1–35.

Hose, R. K., and Danes, Z. F., 1973, Development of the late Mesozoic to early Cenozoic structures in the eastern Great Basin, *in* DeJong, K. A., and Scholten, Robert, eds., Gravity and tectonics: New York, John Wiley & Sons, p. 429–441.

Howard, K. A., 1966, Structure of the metamorphic rocks of the northern Ruby Mountains, Nevada (Ph.D. thesis): New Haven, Conn., Yale Univ., 170 p.

Hubbert, M. K., and Rubey, W. W., 1959, Mechanics of fluid-filled porous solids and its application to overthrust faulting: Geol. Soc. America Bull., v. 70, p. 115–166.

Kehle, R. O., 1970, Analysis of gravity sliding and orogenic translation: Geol. Soc. America Bull., v. 81, p. 1641–1664.

Kerr, J. W., 1962, Paleozoic sequences and thrust slices of the Seetoya Mountains, Independence Range, Elko County, Nevada: Geol. Soc. America Bull., v. 73, p. 439–460.

King, P. B., 1969, Tectonic map of North America: U.S. Geol. Survey, scale 1:5,000,000, 1 sheet.

Kistler, R. W., and Willden, R., 1969, Age of thrusting in the Ruby Mountains, Nevada: Geol. Soc. America Abs. with Programs for 1969, pt. 3 (Rocky Mountains Sec.), p. 40.

Lee, Donald E., Marvin, Richard F., Stern, T. W., and Peterman, Zell E., 1970, Modification of potassium-argon ages by Tertiary Thrusting in the Snake Range, White Pine County, Nevada: U.S. Geol. Survey Prof. Paper 700-D, p. D92–D102.

Misch, P., 1960, Regional structural reconnaissance in central-northeast Nevada and some adjacent areas — Observations and interpretations, *in* Inter. Assoc. Petroleum Geologists Guidebook 11th Ann. Field Conf. Geology of east-central Nevada: p. 17–42.

Misch, P., and Hazzard, J. C., 1962, Stratigraphy and metamorphism of late Precambrian rocks in central-northeast Nevada and adjacent Utah: Am. Assoc. Petroleum Geologists Bull., v. 46, p. 289–344.

Moores, E. M., Scott, R. B., and Lumsden, W. W., 1968, Tertiary tectonics of the White Pine–Grant Range region, east-central Nevada, and some regional implications: Geol. Soc. America Bull., v. 79, p. 1703–1726.

Naeser, C. W., and Faul, H., 1969, Fission-track annealing in apatite and sphene: Jour. Geophys. Research, v. 74, p. 705–710.

Nelson, R. B., 1966, Structural development of northernmost Snake Range, Kern Mountains, and Deep Creek Range, Nevada-Utah: Am. Assoc. Petroleum Geologists Bull., v. 50, p. 921–951.

——1969, Relation and history of structures in a sedimentary succession with deeper metamorphic structures, eastern Great Basin: Am. Assoc. Petroleum Geologists Bull., v. 53, p. 307–339.

Nolan, T. B., 1935, The Gold Hill mining district, Utah: U.S. Geol. Survey Prof. Paper 177, 172 p.

Olson, Richard H., 1956, Geology of Promontory Range, *in* Guidebook to the geology of Utah, no. 11: Utah Geol. and Mineralog. Survey, p. 41–75.

O'Neill, J. M., 1969, Structural geology of the southern Pilot Range, Elko County, Nevada, and Box Elder and Tooele Counties, Utah: Geol. Soc. America, Abs. with Programs for 1969, Pt. 3 (Rocky Mountain Sec.), p. 61.

Oversby, B., 1972, Thrust sequences in the Windermere Hills, northeastern Elko County, Nevada: Geol. Soc. America Bull., v. 83, p. 2677–2688.

Peace, F. S., 1956, History of exploration for oil and gas in Box Elder County, Utah and vicinity, *in* Guidebook to the geology of Utah, no. 11: Utah Geol. and Mineralog. Survey, p. 17–35.

Reed, J. C., Jr., and Zartman, R. E., 1973, Geochronology of Precambrian rocks of the Teton Range, Wyoming: Geol. Soc. America Bull., v. 84, p. 561–582.

Riva, J., 1970, Thrusted Paleozoic rocks in the northern and central Hot Creek Range, northeastern Nevada: Geol. Soc. America Bull., v. 81, p. 2689–2716.

Roberts, R. J., 1968, Tectonic framework of the Great Basin: Missouri Univ. Rolla Tech. Ser., no. 1, p. 101–119.

Roberts, R. J., and Crittenden, M. D., Jr., 1973, Orogenic mechanisms, Sevier orogenic belt, Nevada and Utah, *in* DeJong, K. A., and Scholten, Robert, eds., Gravity and tectonics: New York, John Wiley & Sons, p. 409–428.

Roberts, R. J., Crittenden, M. D., Jr., Tooker, E. W., Morris, H. T., Hose, R. K., and Cheney, T. M., 1965, Pennsylvanian and Permian basins in northwestern Utah, northeastern Nevada and south-central Idaho: Am. Assoc. Petroleum Geologists Bull., v. 49, p. 1926–1956.

Schaeffer, F. E., and Anderson, W. L., 1960, Geology of the Silver Island Mountains, Box Elder and Tooele Counties, Utah, and Elko County, Nevada, *in* Guidebook to the geology of Utah, no. 15: Utah Geol. Soc., 185 p.

Slack, J. F., 1974, Jurassic suprastructure in the Delano Mountains, northeastern Elko County, Nevada: Geol. Soc. America Bull., v. 85, p. 269–272.

Thorman, C. H., 1970, Metamorphosed and nonmetamorphosed Paleozoic rocks in the Wood Hills and Pequop Mountains, northeast Nevada: Geol. Soc. America Bull., v. 81, p. 2417–2448.

Todd, V. R., 1973, Structure and petrology of metamorphosed rocks in central Grouse Creek Mountains, Box Elder County, Utah (Ph.D. thesis): Stanford, Calif., Stanford Univ., 316 p.

Tschanz, L. M., and Pampeyan, E. H., 1970, Geology and mineral deposits of Lincoln County, Nevada: Nevada Bur. Mines Bull., v. 73, 188 p.

Whitebread, D. H., 1966, Snake Range décollement and related structures in the southern Snake Range, eastern Nevada (abs.): Geol. Soc. America Spec. Paper 101, p. 345.

Willden, R., Thomas, H. H., and Stern, T. W., 1967, Oligocene or younger thrust faulting in the Ruby Mountains, northeastern Nevada: Geol. Soc. America Bull., v. 78, p. 1345–1358.

Woodward, L. A., 1964, Structural geology of central northern Egan Range, Nevada: Am. Assoc. Petroleum Geologists Bull., v. 48, p. 22–39.

Woodward, L. A., 1967, Stratigraphy and correlation of late Precambrian rocks of Pilot Range, Elko County, Nevada, and Box Elder County, Utah: Am. Assoc. Petroleum Geologists Bull., v. 51, p. 235–245.

York, Derek, 1966, Least-squares fitting of a straight line: Canadian Jour. Physics, v. 44, p. 1079–1086.

Young, J. C., 1960, Structure and stratigraphy in north-central Schell Creek Range, *in* Intermn. Assoc. Petroleum Geologists Guidebook, 11th Ann. Field Conf., Geology of east-central Nevada: p. 158–172.

MANUSCRIPT RECEIVED BY THE SOCIETY MARCH 29, 1976
REVISED MANUSCRIPT RECEIVED NOVEMBER 10, 1976
MANUSCRIPT ACCEPTED DECEMBER 11, 1976